

Available online at [www.sciencedirect.com](http://www.sciencedirect.com)

SciVerse ScienceDirect

Physics Procedia 41 (2013) 881 – 886

Physics

Procedia

Lasers in Manufacturing Conference 2013

# Simulation of laser beam melting of steel powders using the three-dimensional volume of fluid method

F.-J. Gürtler<sup>a,b,\*</sup>, M. Karg<sup>a,b</sup>, K.-H. Leitz<sup>a,b</sup>, M. Schmidt<sup>a,b</sup><sup>a</sup>Chair of Photonic Technologies, University Erlangen-Nuremberg, Paul-Gordan-Str. 3, 91052 Erlangen, Germany<sup>b</sup>Graduate school in advanced optical technologies (SAOT) Erlangen, Paul-Gordan-Str. 6, 91052 Erlangen, Germany

## Abstract

A transient three-dimensional beam-matter-interaction model was developed to simulate the process dynamics of laser beam melting (LBM) of metals in the powder bed. The simulations were realized by the software OpenFOAM and modified solvers. Based on the continuity equation, the equation of heat conduction and the Navier-Stokes equation the laser material interaction is described. Furthermore, the volume of fluid method is used to characterize the free surfaces of the multi-phase system. These process simulations were performed for steel powders. The parameters were chosen according to those applied in industrial machines and the simulation results show good correlation to experimental data.

© 2013 The Authors. Published by Elsevier B.V. Open access under [CC BY-NC-ND license](http://creativecommons.org/licenses/by-nc-nd/4.0/).

Selection and/or peer-review under responsibility of the German Scientific Laser Society (WLT e.V.)

Keywords: selective laser melting; rapid prototyping; process simulation;

## 1. Introduction

In the last years additive manufacturing (AM) has become more and more important for many industry sectors. By the improvements of laser systems, especially the medium output power, the development from selective laser sintering over the direct metal laser sintering to the laser beam melting (LBM) was possible. In contrast to the two first mentioned methods, in LBM it is possible to use one metal component processing because the used powder is melted completely and no additional material is needed. The generated

---

\* Corresponding author. Tel.: +49-9131-85-23239 ; fax: +49-9131-85-23234 .

E-mail address: [Franz-Josef.Guertler@lpt.uni-erlangen.de](mailto:Franz-Josef.Guertler@lpt.uni-erlangen.de) .

components show due to the complete fusing full density. Also due to the fusing process and the extremely high solidification rate, resulting to a fast cooling rate, the structure underlies a complete new formation.

In order to optimize the LBM process and to avoid unwanted porosity there is an increasing interest in understanding the process dynamics of laser beam melting, especially the mechanisms of defect formation. For the description of the process dynamics of LBM a simulation model is necessary which includes energy input, phase transition as well as thermo and fluid dynamics. Indeed some numerical models exist in this field of LBM, but they make strong simplifications regarding the geometry or the physical effects [Wakai, 2006, Wang et al., 2002, Chen and Zhang, 2006 and Zaeh et al., 2009]. So a transient three-dimensional numerical simulation model was developed by using the volume of fluid method to elucidate the melting and resolidification problem of the LBM process by an explicit wetting.

## 2. Simulation Model

### 2.1. Physical Model

The simulations base on the computational fluid dynamics toolbox *OpenFOAM* (Open Field Operation And Manipulation, ©OpenCFD Limited) which is a C++ toolbox for the numerical solution of continuum mechanical dynamical problems. The software allows modifying standard solvers like for heat transfer and multiphase flow to model the specific physical phenomena of laser beam melting. During the last years specific solvers have been developed at the Chair of Photonic Technologies to simulate the interaction between laser and material for different material processing techniques [Geiger et al., 2009, Otto and Schmidt, 2010, Otto et al., 2011 and Leitz et al., 2012]. For this many physical effects had to be coupled. The energy flux in the fluid and solid phases are considered as a system of coupled nonlinear partial differential equations. The flow characteristic of the molten steel is described as an incompressible fluid by the Navier-Stokes equation [Versteeg and Malalasekera, 2006]. The free surface of the molten steel is described by the volume of fluid (VOF) method [Hirt and Nichols, 1981 and Ferziger and Peric, 2008]. The energy flux and the physics of the phase transformation are considered. The heat of melting and evaporation are included in the model [Ki et al., 2001]. By this rich in detail configured simulation model the shape of the melt pool and therefore the hydrodynamics can be determined. The most important parts of the laser beam melting are the heat flux, the surface and the interaction of the material with the laser which are described detailed by the following equations. The physical properties and process parameters are listed in Table 1 and Table 2.

Table 1. Process parameters

Process parameter	symbol	unit	value
Laser power	$P_L$	W	200
Focus radius	$w_0$	$\mu\text{m}$	50
Feed velocity	$v_0$	m/s	1
Wavelength	$\lambda$	nm	1064
Scan spacing	$s$	$\mu\text{m}$	100
Powder diameter	$d$	$\mu\text{m}$	30

Table 2. Physical properties

Physical property	symbol	unit	value
Density of steel	$\rho$	Kg/m <sup>3</sup>	7840
Specific heat of liquid and solid steel	$c_S / c_L$	J/(Kg·K)	460
Thermal conductivity of steel	$k$	W/(m·Kg)	50
Kinematic viscosity of molten steel	$\nu$	m <sup>2</sup> /s	1·10 <sup>-6</sup>
Melting temperature of steel	$T_M$	K	1808
Vaporization temperature	$T_V$	K	3134
Enthalpy of fusion	$H_M$	KJ/kg	277
Enthalpy of vaporization	$H_V$	KJ/kg	6340
Surface tension coefficient	$\sigma$	N/m	1.79
Complex refraction index ( $\lambda = 1.064 \mu\text{m}$ )	$n+k\cdot i$	-	3.23 + 4.35·i

## 2.2. Governing Equations

The evolution of the temperature field is significantly influenced by the phase transitions. The fusion and resolidification of the metal is considered in the dynamic. To map the melting and evaporation enthalpy the heat conduction equation is formulated in the energy form [Dowden, 2009]:

$$\frac{\partial}{\partial t}(\rho \cdot H) + \nabla \cdot (\rho \cdot \vec{u} \cdot H) - \nabla \cdot (\lambda \cdot \nabla T) = Q_A$$

The solution of this problem bases on an iterative method, in which the enthalpies are included more correctly at every calculation step [Kohl et al., 2012].

The fluid dynamic is based on a multi-phase fluid dynamic solver of *OpenFOAM* and is solved by the PISO (Pressure Implicit with Splitting of Operators) scheme and is described by the incompressible Navier-Stokes equation [Dowden, 2001 and Bristeau et. al, 1987]

$$\rho \frac{\partial \vec{u}}{\partial t} + \rho \vec{u} \cdot \nabla \vec{u} = -\rho \nabla p + \eta \Delta \vec{u}$$

and mass conservation equation

$$\frac{\partial \rho}{\partial t} + \nabla(\rho \vec{u}) = 0$$

The flow of the solid phase is not possible, so the speed is constant zero.

The laser beam is simulated as a volume heat source with Gaussian distribution. The absorption coefficient depends on the angle of incidence and thus it is given by the Fresnel equations [Hügel, 1995]. The attenuation of the energy of the laser beam in the metal follows the Beer-Lambert law [Demtröder, 2006].

## 2.3. Specification of Geometry and Mesh of the Simulation

To reduce the complexity of the simulation a simple configuration of the process has been chosen. So the powder particles are represented by spheres with a uniform diameter of  $30 \mu\text{m}$ . Furthermore, the powder bed

is a face-centered cubic system. To reduce the relative density of the powder to a realistic scale (around 60% content) some spacing between the particle spheres is introduced. For a realistic modeling of the powder geometry, the mesh on the powder surface is locally refined. The refinement degree is a trade-off between too angular powder particles and too large calculation time because of a high number of cells. So there are numerical connections of the spheres which increase the heat conduction between the particles. All this matches the characteristics of the used powders.

### 3. Results and Discussion

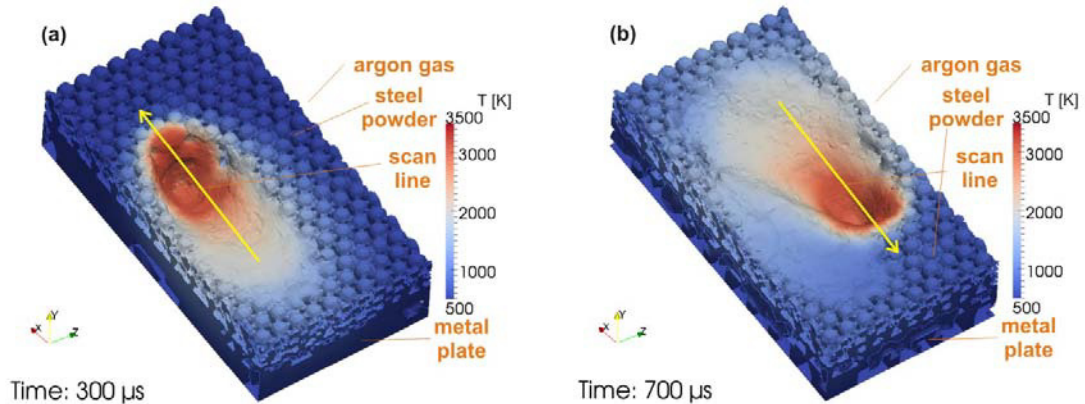


Fig. 1. (a) Overview of the process after a single scan line ( $t = 300 \mu s$ );  
 (b) Overview of the process after a second scan line ( $t = 700 \mu s$ ) in distance of  $100 \mu m$  to the first line;  
 The process parameters are:  $P_L = 200 W$ ,  $\lambda = 1064 nm$ ,  $w_0 = 50 \mu m$ ,  $v_0 = 1 m/s$ .

For the simulation a small experimental setup is chosen to limit the calculation time. So a box ( $600 \mu m \times 320 \mu m \times 200 \mu m$ ) is analyzed in which the relevant phenomena of the process can be seen. The boundaries are open for the material and energy flow, only the bottom side has a constant temperature of  $T = 500 K$  to model the influence of the pre-heated powder bed. In Fig. 1 an exemplary process at standard processing parameters is displayed at different time steps. The laser beam is moving along a line of  $400 \mu m$ . The line spacing is  $s = 100 \mu m$ , the feed rate is  $v_0 = 1 m/s$ , the laser power is  $P_L = 200 W$ , the wavelength is

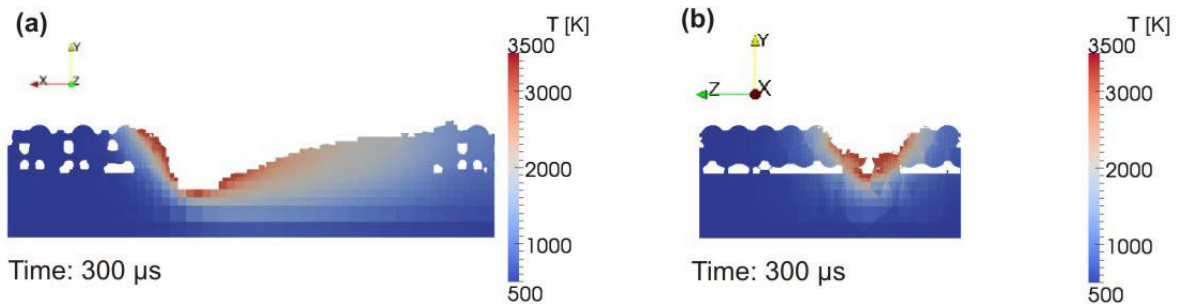


Fig. 2. (a) Slice of the powder bed along the laser feed direction through the focal spot ( $t = 300 \mu s$ );  
 (b) Slice of the powder bed orthogonal to the laser feed direction through the focal spot ( $t = 300 \mu s$ );  
 The process parameters are:  $P_L = 200 W$ ,  $\lambda = 1064 nm$ ,  $w_0 = 50 \mu m$ ,  $v_0 = 1 m/s$ ,  $s = 100 \mu m$ .

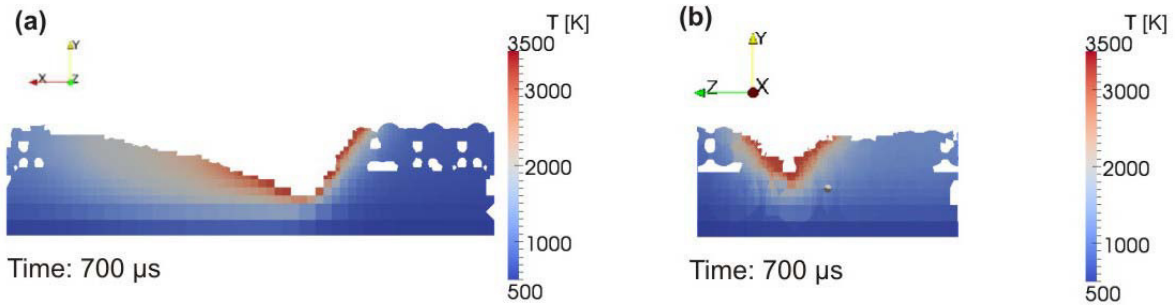


Fig. 3. (a) Slice of the powder bed along the laser feed direction through the focal spot ( $t = 700 \mu s$ );  
 (b) Slice of the powder bed orthogonal to the laser feed direction through the focal spot ( $t = 700 \mu s$ );  
 The process parameters are:  $P_L = 200 W$ ,  $\lambda = 1064 nm$ ,  $w_0 = 50 \mu m$ ,  $v_0 = 1 m/s$ ,  $s = 100 \mu m$ .

$\lambda = 1064 nm$  and the laser beam radius is set to  $w_0 = 50 \mu m$ . The powder particles have a diameter of  $d = 30 \mu m$  and are located over a compact steel plate. To reduce the numerical connections because of the coarse mesh a separation distance of around  $2 \mu m$  is inserted in all directions.

Fig. 1 demonstrates that the simulation model can achieve realistic results. It displays the melting of the powder particles, the wetting of the liquid to the solid material and the solidification of the melt. After one scan (Fig. 1a) a significant coalescence of the powder and the plate already exists with a smooth surface. Fig. 1b shows the results of a second scan line. The maximum of the temperature field is limited by the evaporation. In the simulation the whole absorptance of the laser power in the material ranges between 60% and 70% in each time step. In both scans the metal plate has been molten for a deeper connection of the bead which can especially be seen in Fig. 2a and b. The slices of the box after the laser absorption are displayed in Fig. 3a and b. The compact layer has a realistic height of around 60% of the powder layer. The bead of the second scan line is much deeper as the first one at the beginning. A reason can be the flow of the melt to the back of the heating area.

Also the simulation model can image defects. Fig. 4a displays a metallurgical grinding of porosity defects at false parameters. The simulation with too small power can produce similar defects (Fig. 4b). Here the fusing of the powder in the metal plate is not perfect. There are some holes between the scan lines, metal plate and powder.

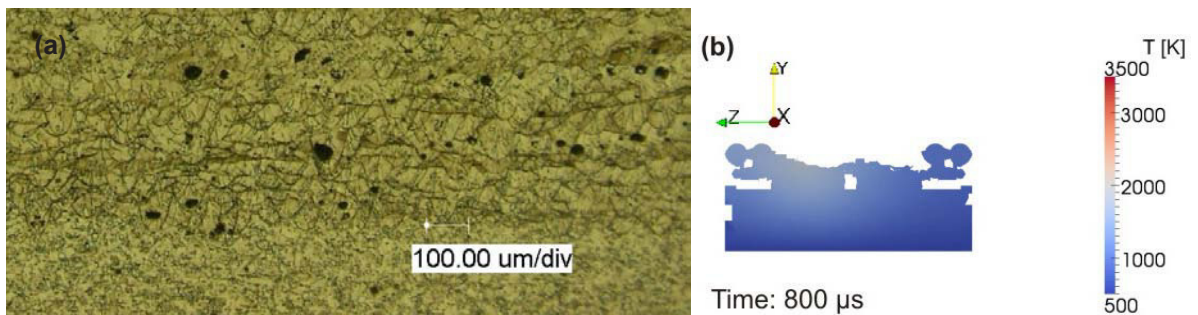


Fig. 4. Comparison of porosity in experiment and simulation:  
 (a) Experiment with  $P_L = 75 W$ ,  $w_0 = 10 \mu m$ ,  $v_0 = 0.25 m/s$ ,  $s = 50 \mu m$ : Black areas are wholes without material;  
 (b) Simulation with  $P_L = 100 W$ ,  $w_0 = 20 \mu m$ ,  $v_0 = 1 m/s$ ,  $s = 100 \mu m$ : White areas are wholes without material;  
 The other process parameters are:  $\lambda = 1064 nm$ .

## 4. Summary and Outlook

In this contribution a numerical simulation model for LBM has been presented describing melting, wetting and solidification phenomena. The model is able to reproduce the fundamental properties of the laser beam melting process. The effects of the powder-layer thickness, moving heat source intensity, scan spacing and scanning velocity on the process dynamics can be shown. Realistic results for process dynamics in LBM are presented by using the parameters of industrial machines like the Renishaw AM125 or the Realizer SLM 50.

## Acknowledgements

The authors gratefully acknowledge the funding of the Erlangen Graduate School in Advanced Optical Technologies (SAOT) by the German National Science Foundation (DFG) in the frame work of the excellence initiative.

## References

- Wakai, F., 2006. Modeling and Simulation of Elementary Processes in Ideal Sintering. *Journal of the American Ceramic Society* 89 [5], p. 1471–1484.
- Wang, X. C., Laoui, T., Bonse, J., Kruth, J. P., Lauwers, B., Froyen, L., 2002. Direct Selective Laser Sintering of Hard Metal Powders: Experimental Study and Simulation. *The International Journal of Advanced Manufacturing Technology* 19, p. 351–357.
- Chen, T., Zhang, Y., 2006. Three-Dimensional Modeling of Selective Laser Sintering of Two-Component Metal Powder Layers. *Journal of Manufacturing Science and Engineering* 128, p. 299–306.
- Zaeh, M. F., Branner, G., Krol, T.A., 2009. A three dimensional FE-model for the investigation of transient physical effects in Selective Laser Melting. *Innovative Developments in Design and Manufacturing – Adv. Res. in Vir. and Rap. Pro.*
- Geiger, M., Leitz, K.-H., Koch, H., Otto, A., 2009. A 3D transient model of keyhole and melt pool dynamics in laser beam welding applied to the joining of zinc coated sheets. *Production Engineering* 3 [2], p. 127–136.
- Otto A., Schmidt, M., 2010. Towards a Universal Numerical Simulation Model for Laser Material Processing. *Physics Procedia* 5, p. 35–46.
- Otto, A., Koch, H., Leitz, K.-H., Schmidt, M., 2011. Numerical Simulations – A Versatile Approach for Better Understanding Dynamics in Laser Material Processing. *Physics Procedia* 12, p. 11–20.
- Leitz, K.-H., Koch, H., Otto, A., Schmidt, M., 2012. Numerical Simulation of Process Dynamics During Laser Beam Drilling With Short Pulses. *Applied Physics A* 106, p. 885–891.
- Versteeg, H. K., Malalasekera, W., 2006. *An Introduction to Computational Fluid Dynamics - The Finite Volume Method*. Pearson Education Limited, Harlow.
- Hirt, C. W., Nichols, B. D., 1981. Volume of Fluid (VOF) Method for the Dynamics of Free Boundaries. *Journal of Computational Physics* 39, p. 201–225
- Ferziger, J., Peric, M., 2008. *Numerische Strömungsmechanik*. Springer, Berlin.
- Ki, H., Mohanty, P. S., Mazumder, J., 2001. Modelling of high-density laser-material interaction using fast level set method. *Journal of Physics D: Applied Physics* 34, p. 364–372.
- Dowden, J.M., 2009. *The Theory of Laser Materials Processing*. Springer, Wiesbaden.
- Kohl, S., Leitz, K.-H., Schmidt, M., 2012. Transient Numerical Simulation of CO<sub>2</sub> Laser Fusion Cutting of Metal Sheets – Simulation Model and Process Dynamics. *Proceedings of the 37th MATADOR Conference, Manchester*, Springer, p. 403.
- Dowden, J.M., 2001. *The Mathematics of Thermal Modeling*. Chapman & Hall/CRC, Boca Raton.
- Bristeau, M.O., Glowinski, R., Priaux, J., 1987. *Comput. Phys. Rep.* 6.
- Hügel, H., Graf, T., 1995. *Laser in der Fertigung*. Vieweg+Teubner Verlag, Berlin.
- Demtröder, E., 2006. *Experimentalphysik 2, Elektrizität und Optik*. Springer, Berlin.